Supporting Information

Table of contents

Figure S1. Schematic representation of the peptide bond formation using HOBt/EDC approach.

Figure S2. Schematic representation of the peptide bond formation using isobutylchloroformiate as a coupling reagent.

Figure S3. Resonance forms of the dithiocarbamic –NCSS$^-$ moiety.

Figure S4. Different ways of metal-sulfur binding in dithiocarbamate complexes: symmetrical bidentate (a), asymmetrical bidentate (b) and monodentate (c).

Figure S5. ^{1}H-NMR spectra of IT01 in DMSO-d_6 over 48 h.

Figure S6. ^{1}H-NMR spectra of IT01 in acetone-d_6 over 24 h.

Figure S7. [^{1}H,^{13}C]-HMBC spectrum of IT01 in acetone-d_6.

Figure S8. Crystal packing of IT05·pentane viewed along the b crystallographic axis.

Figure S9. Depiction of intermolecular contacts between two symmetry related molecules of IT05·pentane. Symmetry code ' = 1/2-x; 1/2+y; z.

Figure S10. Crystal packing of IT03/IT04 acetone solvate viewed along the b crystallographic axis.

Figure S11. X-ray diffraction structure of Z-L-Pro-Aib-O*t*Bu with atom numbering (only one position for the disordered C1G atom is shown; H-atoms have been omitted for clarity), characterized by a *cis* configuration of the Z-L-Pro urethane bond [the value of the OU-C0-N1-C1A torsion angle being -17.5(6)°], a not uncommon observation for urethane-protected Pro derivatives. The peptide backbone features a *semi*-extended conformation for the Pro residue [ϕ,ψ = -60.0(5)°, +168.8(3)°] while right-handed helical for Aib [ϕ,ψ = -53.1(5)°, -31.8(5)°]. Such a conformation is closely matched by the L-Pro-Aib segment in the structure of the racemate IT03/IT04. In the packing mode, an intermolecular H-bond is observed between the (peptide) N2-H group and the (-*x*, 1/2+*y*, 3/2-*z*) symmetry equivalent of the (urethane carbonyl) O0=C0 group, linking molecules related by a twofold screw axis along the *b* direction.

Figure S12. Electronic spectra of IT03 (50 μM) recorded in DMSO at 25°C for 24 h.

Figure S13. Electronic spectra of IT03 (50 μM) recorded in deionized water at 25°C for 24h.

Figure S14. Electronic spectra of IT03 (50 μM) recorded in saline solution (NaCl 0.9% w/v) at 25°C for 24 h.

Figure S15. Electronic spectra of IT03 (50 μM) recorded in PBS buffer pH=7.4 at 25°C over 4 h.

Figure S16. Electronic spectra of IT03 (30 μM) in PBS added of 20% v/v complete medium (RPMI-1640 medium supplemented with 10% fetal calf serum) at 25°C for 24 hours.

Figure S17. Inhibition of PARP-1 activity by the test compounds at different concentrations (from 10 to 0.01 μM). For the assay each compound was incubated for 1 h with 0.5 U of purified protein.

Figure S18. Electronic spectrum of BSA and IT03 (equimolar, 30 μM) in PBS at 25°C over 24h.

Figure S19. CD spectra of BSA incubated with IT03 at different molar ratios (from 0 to 3) in PBS at 25°C.

Figure S20. Fluorescence spectra of BSA (15 µM) in presence of IT03 (15 µM) in PBS at 25°C over 24h.

Figure S21. Intensity fluorescence at the λ_{em} maximum (349 nm) of BSA alone (■) and when incubated with IT03 as a function of time (●, 0-6 h)

Figure S22. Fluorescence spectra of BSA (15 µM) in presence of IT03 at different molar ratios (from 0 to 3) soon after mixing, in PBS at 25°C.

Figure S23. Intensity fluorescence at the λ_{em} maximum (349 nm) of BSA alone (■) and when incubated with IT03 at different IT03/BSA molar ratios (From 0.3 to 3; ●).

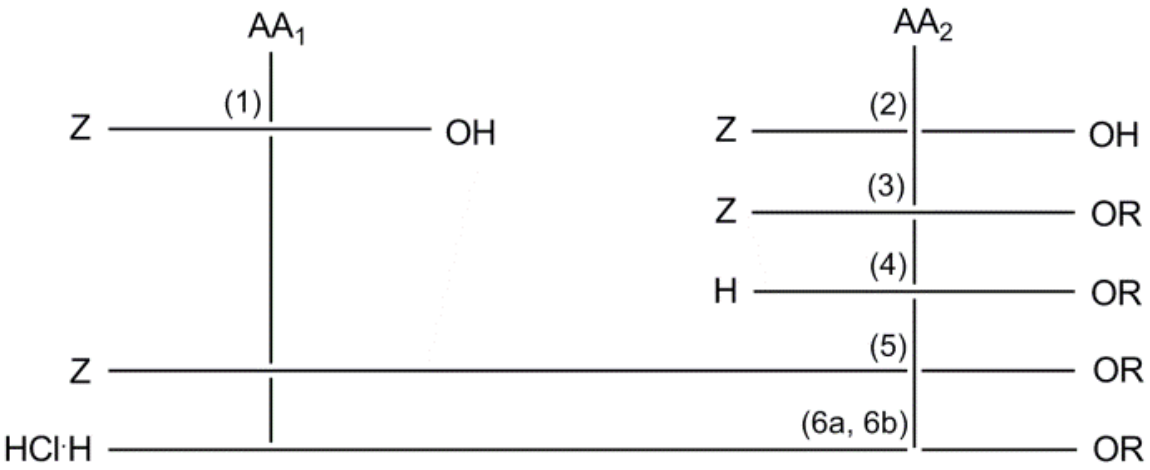

Scheme S1. Synthetic scheme for the preparation of hydrochloride dipeptide esters P1-P5 (AA_1= Sar, L/D-Pro; AA_2=L/D-Ala, Aib; R= O*t*Bu, OTEG). (1) and (2) Z-OSu, triethylamine, CH_3CN/H_2O; (3) –OtBu: isobutene, H_2SO_4 cat., CH_2Cl_2; -OTEG: EDC/DMAP/HOBt* (Figure S1), triethylen glycol monomethyl ether, CH_2Cl_2; (4) H_2, Pd/C (10% w/w), methanol; (5) for the Sar-derivatives isobutyl chloroformiate (Figure S2), *N*-methylmorpholine, tetrahydrofurane; for the Pro-derivatives EDC, HOBt, diethylisopropylamine, dichloromethane; (6a) H_2, Pd/C, methanol; (6b) HCl/diethylether.

*1-ethyl-3-(3-dimethylaminopropyl)carbodiimide/4-dimethylaminopyridine/Hydroxybenzotriazole

Table S1. Thermogravimetric (TG) and differential scanning calorimetric (DSC) data.

Compound	Weight loss (%)		DSC
	Found	Calculated	Peak temperature [°C] (process*)
IT01	67.95	69.61	158.0 (endo); 499.4 (exo)
IT02	67.90	69.61	151.0 (endo); 469.4 (exo)
IT03	72.00	71.38	113.7 (endo); 439.7 (exo)
IT04	71.89	71.38	178.0 (endo); 436.7 (exo)
IT05	73.82	72.61	122.6 (endo); 493.7 (exo); 542.1 (exo)

*endo/exo=endothermic/exothermic

Table S2. Selected IR frequencies of the starting dipeptides P1-P5 and the corresponding gold(III) dithiocarbamato derivatives IT01-IT05.

	Vibrational mode [cm^{-1}]									
	ν NH	$\nu_{a/s}$ NH_2^+	ν C=O	amide I	ν N-CSS	Amide II	Amide III	$\nu_{a/s}$ SCS	$\nu_{a/s}$ SAuS	$\nu_{a/s}$ BrAuBr
P1	3332	2763	1735	1669	-	1564	1266	-	-	-
IT01	3317	-	1733	1668	1564[a]		1219	1003/ 567	419/ 380	251/ 229
P2	3332	2766	1735	1669	-	1564	1266	-	-	-
IT02	3311	-	1732	1668	1563[a]		1218	1003/ 566	419/ 380	251/ 228
P3	3430	2744	1733	1678	-	1551	1256	-	-	-
IT03	3341	-	1730	1680	1553[a]		1247	1000/ 535	410/376	252/222
P4	3437	2744	1733	1678	-	1551	1256	-	-	-
IT04	3363		1732	1680	1549[a]		1241	991/ 533	410/ 376	251/ 222
P5	3193	2762	1739	1684	-	1554	1256	-	-	-
IT05	3290	-	1735	1683	1576	1549	1253	1022/ 569	412/ 390	250/ 226

[a] $\nu_{N\text{-}CSS}$ and amide II are overlapped.

The main signals generated by the peptide chains are the vibration mode of the amide-proton bond ($\nu_{N\text{-}H}$) at 3550-3200 cm^{-1} (Amide A band), and the three bands characteristic of the C(O)NH function, resulting from the combination of the ν(C=O), δ(N-H) and ν(C-N) vibration modes (referred to as amide I, II and III).

With respect to the formation of the gold(III) dithiocarbamato complexes, there are three main diagnostic regions:

- the 1580-1450 cm^{-1} region, primarily associated with the ν(N-CSS) vibration mode ("thioureide" band);
- the 1060-940 cm^{-1} region, associated with the ν(S-C-S) vibration modes;
- the 420-350 cm^{-1} region, associated with the ν(M-S) vibration modes.

Upon complex formation, the deprotonation step of the HCl·dipeptide to form the corresponding dithiocarbamato ligand causes the disappearance of the signal at 2766-2736 cm^{-1} of the $\nu_{a/s}(NH_2^+)$ vibration mode, and the appearance of both the ν(N-CSS) band at 1580-1450 cm^{-1} (somewhat overlapped to amide II band) and the ν_a(S-C-S) band at 1060-940 cm^{-1}.

As described by Chatt *et al.,*[39] the dithiocarbamato moiety is characterized by a strong delocalization of the electrons, being described by three main resonance structures (Figure S3). The position of the ν(N-CSS) bands recorded for our compounds is consistent with the presence of a carbon-nitrogen bond order which lies between a single bond (ν=1350-1250 cm^{-1}) and a double bond ($\tilde{\nu}$ =1690-1640 cm^{-1}).[40] This is in agreement with a relevant contribution to the final structure

of the resonance form III reported in Figure S3, characterized by a symmetric chelated coordination of the dithiocarbamato function to the gold(III) metal center.[52] Likewise, the presence of a single band for the ν_a(S-C-S) at 1022-991 and the ν_s(S-C-S) at 569-533 cm^{-1} validates a bidentate symmetric coordination of the ligand to the metal center (Figure S4).[53] In the Far FT-IR region, the formation of a symmetrically-chelated dithiocarbamato is further confirmed by the position of the metal-sulfur stretching vibrations $\nu_{a/s}$(S-Au-S) at 419-410/390-376 cm^{-1}, in agreement with previously reported data.[52, 54] The bands related to the *cis*-coordinated halides $\nu_{a/s}$(Br-Au-Br) set at 252-250/229-220 cm^{-1}.[52, 54-55]

Table S3. ^{13}C NMR spectral data of the starting dipeptides P1-P5 (HCl·H-AA_1-AA_2-OR: AA_1= Sar, L/D-Pro; AA_2=D/L-Ala, Aib; R= -*t*Bu, TEG) and the corresponding gold(III)-dithiocarbamato derivatives IT01-IT05 ([$Au^{III}Br_2$(dtc-AA_1-AA_2-OR]) (DMSO-d_6, 298 K, 75.48 MHz).

Compound	δ (^{13}C) [ppm]			
	-OR	AA_1	AA_2	*C*-SS
	R=*t*Bu	**AA_1=Sar**	**AA_2=L-Ala**	
P1	27.36(-C(**C**H_3)$_3$)	32.40(N- **C**H_3)	16.75 (β- **C**H_3)	-
	80.58(-**C**(CH_3)$_3$)	48.53(N- **C**H_2)	48.29 (α-**C**H)	
		164.86 (**C**=O)	171.27 (**C**=O)	
IT01*	28.35(-C(**C**H_3)$_3$)	40.5 (N-**C**H_3)	18.34 (β- **C**H_3)	198.2
	82.36(-**C**(CH_3)$_3$)	55.5 (N- **C**H_2)	50.35 (α-**C**H)	
		164.72 (**C**=O)	172.54 (**C**=O)	
	R= *t*Bu	**AA_1=Sar**	**AA_2=D-Ala**	-
P2	27.28(-C(**C**H_3)$_3$)	32.41(N- **C**H_3)	16.76(β- **C**H_3)	
	80.55(-**C**(CH_3)$_3$)	48.52(N- **C**H_2)	48.29(α-**C**H)	
		164.87 (**C**=O)	171.22 (**C**=O)	
IT02*	27.69(-C(**C**H_3)$_3$)	39.9 (N- **C**H_3)	17.67 (β- **C**H_3)	197.72
	81.70(-**C**(CH_3)$_3$)	54.83 (N- **C**H_2)	49.68 (α-**C**H)	
		163.81 (**C**=O)	171.88 (**C**=O)	
	R= *t*Bu	**AA_1=L-Pro**	**AA_2=Aib**	-
P3	27.13(-C(**C**H_3)$_3$)	23.28 (**C**H_2^4)	55.69 **C**(CH_3)$_2$	
			24.41 (**C**H_3)	
	79.65(-**C**(CH_3)$_3$)	29.59 (**C**H_2^3)	172.15 (**C**=O)	
		45.32 (**C**H_2^5)		
		58.07 (**C**H^2)		
		167.15 (**C**=O)		
IT03*	28.00(-C(**C**H_3)$_3$)	23.09 (**C**H_2^4)	25.01 (**C**H_3)	190.22
			57.28 **C**(CH_3)$_2$	
			172.84 (**C**=O)	
	80.98(-**C**(CH_3)$_3$)	30.84 (**C**H_2^3)		
		52.10 (**C**H_2^5)		
		64.87 (**C**H^2)		
		166.69 (**C**=O)		
	R= *t*Bu	**AA_1=D-Pro**	**AA_2=Aib**	-
P4	27.19(-C(**C**H_3)$_3$)	23.56 (**C**H_2^4)	24.50 (**C**H_3)	
			55.70 **C**(CH_3)$_2$	
			172.06 (**C**=O)	
	79.65(-**C**(CH_3)$_3$)	29.67 (**C**H_2^3)		
		45.55 (**C**H_2^5)		
		58.26 (**C**H^2)		
		167.75 (**C**=O)		
IT04*	27.97(-C(**C**H_3)$_3$)	23.16 (**C**H_2^4)	24.95 (**C**H_3)	190.21
			57.44 **C**(CH_3)$_2$	
	81.10(-**C**(CH_3)$_3$)	30.80 (**C**H_2^3)	172.96 (**C**=O)	
		52.08 (**C**H_2^5)		
		64.92 (**C**H^2)		

		166.94 (**C**=O)		
	R=TEG	**AA_1=Sar**	**AA_2=Aib**	
P5	57.26 (O-**C**H_3) 63.19 (**C**H_2^1)	31.84 (N-**C**H_3)	23.39(β-**C**H_3) 54.77 **C**$(CH_3)_2$ 172.52 (**C**=O)	
	67.44 (**C**H_2^2)	47.94 (N-**C**H_2)		
	68.8-70.7 (**C**$H_2^{3,4,5,6}$)	163.80 (**C**=O)	172.52 (**C**=O)	
IT05*	58.52 (O**C**H_3) 64.52 (**C**H_2^1) 69.25 (**C**H_2^2) 70.8-71.2 (**C**H_2 ^{3,4,5,6})	39.86 (N**C**H_3) 54.84 (N**C**H_2) 163.54 (**C**=O)	24.86(β-**C**H_3) 57.00 **C**$(CH_3)_2$ 173.63 (**C**=O)	197.3

* acetone-d_6 (recorded in such a solvent due to signal overlapping with DMSO resonances).

Table S4. Summary of X-ray crystallographic data for IT05·pentane.

Empirical formula	$C_{20}H_{39}AuBr_2N_2O_6S_2$
Formula weight	824.44
Colour, habit	Yellow, block
Crystal size, mm	0.07x0.04x0.04
Crystal system	Orthorhombic
Space group	*P*bcn
a, Å	22.15(2)
b, Å	9.599(9)
c, Å	25.88(2)
α, deg.	90
β, deg.	90
γ, deg.	90
V, Å^3	5503(8)
Z	8
T, K	293(2)
ρ (calc), Mg/m^3	1.990
μ, mm^{-1}	8.440
θ range, deg.	1.82 to 20.75
No.ofrflcn/unique	9221 / 2636
GooF	1.028
*R*1	0.0877
*wR*2	0.1774

$R1 = \Sigma||F_O|-|F_C||/\Sigma|F_O|$, $wR2 = [\Sigma[w(F_O^2-F_C^2)^2]/\Sigma[w(F_O^2)^2]]^{½}$, $w = 1/[\sigma^2(F_O^2) + (aP)^2 + bP]$, where $P = [\max(F_O^2,0) + 2F_C^2]/3$

Table S5. Selected bond lengths (Å) and angles (°) for IT05·pentane.

Au-Br(1)	2.429(4)	C(1)-N(1)	1.32(3)
Au-Br(2)	2.431(5)	C(4)-O(1)	1.27(3)
Au-S(1)	2.310(9)	C(4)-N(2)	1.33(3)
Au-S(2)	2.306(9)	C(8)-O(2)	1.21(4)
C(1)-S(1)	1.78(3)	C(8)-O(3)	1.36(4)
C(1)-S(2)	1.71(3)		
Br(1)-Au-Br(2)	94.0(2)	S(1)-C(1)-S(2)	108(2)
S(1)-Au-S(2)	75.7(3)	C(1)-S(1)-Au	87(1)
Br(1)-Au-S(1)	96.1(2)	C(1)-S(2)-Au	89(1)
Br(2)-Au-S(2)	94.1(2)		

Table S6. Crystallographic data and structure refinement for the racemate IT03/IT04 [$Au^{III}Br_2$(dtc-L,D-Pro-Aib-O*t*Bu)] acetone solvate.

Identification code	mc181fl	
Empirical formula	$C_{14}H_{23}AuBr_2N_2O_3S_2$ x C_3H_6O	
Formula weight	746.33	
Temperature	293(2) K	
Wavelength	0.71070 Å	
Crystal system	Orthorhombic	
Space group	Pbca	
Unit cell dimensions	a = 16.5424(6) Å	α= 90°.
	b = 11.7649(4) Å	β= 90°.
	c = 26.3963(7) Å	γ = 90°.
Volume	5137.2(3) $Å^3$	
Z	8	
Density (calculated)	1.930 Mg/m^3	
Absorption coefficient	9.024 mm^{-1}	
F(000)	2864	
Crystal size	0.50 x 0.40 x 0.15 mm^3	
Theta range for data collection	3.09 to 26.37°.	
Index ranges	-20<=h<=20, -14<=k<=14, -25<=l<=27	
Reflections collected	9339	
Independent reflections	3000 [R(int) = 0.0488]	
Completeness to theta = 26.37°	57.1 %	
Absorption correction	Semi-empirical from equivalents	
Max. and min. transmission	1.00000 and 0.20457	
Refinement method	Full-matrix least-squares on F^2	
Data / restraints / parameters	3000 / 158 / 285	
Goodness-of-fit on F^2	1.255	
Final R indices [I>2sigma(I)]	R_1 = 0.0871, wR_2 = 0.1526	
R indices (all data)	R_1 = 0.1151, wR_2 = 0.1610	
Largest diff. peak and hole	0.783 and -1.024 e.$Å^{-3}$	

Table S7. Selected bond lengths (Å) and angles (°) for the racemate IT04 [$Au^{III}Br_2$(dtc-L,D-Pro-Aib-O*t*Bu)].

Au-Br(1)	2.420(3)	C(1)-N(1)	1.28(2)
Au-Br(2)	2.435(3)	C(6)-O(1)	1.23(2)
Au-S(1)	2.313(6)	C(6)-N(2)	1.32(2)
Au-S(2)	2.307(7)	C(10)-O(2)	1.25(3)
C(1)-S(1)	1.71(2)	C(10)-O(3)	1.29(3)
C(1)-S(2)	1.74(2)		
Br(1)-Au-Br(2)	93.64(12)	S(1)-C(1)-S(2)	110.3(12)
S(1)-Au-S(2)	75.7(2)	C(1)-S(1)-Au	87.1(8)
Br(1)-Au-S(1)	95.77(18)	C(1)-S(2)-Au	86.8(8)
Br(2)-Au-S(2)	94.93(18)		

Table S8. Crystallographic data and structure refinement for Z-L-Pro-Aib-O*t*Bu.

Identification code	**Z-L-Pro-Aib-O*t*Bu**	
Empirical formula	C21 H30 N2 O5	
Formula weight	390.47	
Temperature	293(2) K	
Wavelength	1.54178 Å	
Crystal system	Orthorhombic	
Space group	P 21 21 21	
Unit cell dimensions	a = 10.050(2) Å	α= 90°.
	b = 10.460(2) Å	β= 90°.
	c = 21.305(3) Å	γ = 90°.
Volume	2239.6(7) $Å^3$	
Z	4	
Density (calculated)	1.158 Mg/m^3	
Absorption coefficient	0.674 mm^{-1}	
F(000)	840	
Crystal size	0.50 x 0.35 x 0.20 mm^3	
Theta range for data collection	4.15 to 59.97°.	
Index ranges	-1<=h<=11, 0<=k<=11, 0<=l<=23	
Reflections collected	2158	
Independent reflections	2121 [R(int) = 0.1078]	
Completeness to theta = 59.97°	99.9 %	
Max. and min. transmission	0.8770 and 0.7293	
Refinement method	Full-matrix-block least-squares on F^2	
Data / restraints / parameters	2121 / 4 / 250	
Goodness-of-fit on F^2	0.992	
Final R indices [I>2sigma(I)]	R1 = 0.0611, wR2 = 0.1612	
R indices (all data)	R1 = 0.0774, wR2 = 0.1735	
Absolute structure	-0.1(5)	

parameter	
Largest diff. peak and hole	0.258 and -0.174 e.Å^{-3}

Table S9. Bond lengths [Å] and angles [°] for Z-L-Pro-Aib-O*t*Bu.

C01-C02	1.39
C01-C06	1.39
C01-C07	1.491(5)
C02-C03	1.39
C03-C04	1.39
C04-C05	1.39
C05-C06	1.39
C07-OU	1.421(5)
OU-C0	1.335(5)
C0-O0	1.231(5)
C0-N1	1.325(5)
N1-C1D	1.456(6)
N1-C1A	1.464(5)
C1A-C1	1.523(6)
C1A-C1B	1.528(6)
C1B-C1G	1.480(8)
C1B-C1G'	1.487(8)
C1G-C1D	1.499(8)
C1G'-C1D	1.497(8)
C1-O1	1.230(5)
C1-N2	1.345(5)
N2-C2A	1.444(6)
C2A-C2B2	1.519(6)
C2A-C2B1	1.536(6)
C2A-C2	1.536(6)
C2-O2	1.204(5)
C2-OT	1.335(5)
OT-CT1	1.481(5)
CT1-CT2	1.501(8)
CT1-CT4	1.501(8)
CT1-CT3	1.507(8)
C02-C01-C06	120
C02-C01-C07	122.4(3)
C06-C01-C07	117.6(3)
C01-C02-C03	120
C02-C03-C04	120
C05-C04-C03	120
C04-C05-C06	120
C05-C06-C01	120
OU-C07-C01	109.0(3)
C0-OU-C07	116.0(3)

O0-C0-N1	124.8(4)
O0-C0-OU	123.3(4)
N1-C0-OU	111.8(3)
C0-N1-C1D	122.1(4)
C0-N1-C1A	122.6(4)
C1D-N1-C1A	112.3(3)
N1-C1A-C1	110.3(3)
N1-C1A-C1B	102.9(3)
C1-C1A-C1B	112.2(4)
C1G-C1B-C1A	106.7(5)
C1G-C1B-C1G'	28.6(7)
C1A-C1B-C1G'	103.9(5)
C1B-C1G-C1D	107.9(6)
C1D-C1G'-C1B	107.6(6)
N1-C1D-C1G'	103.9(5)
N1-C1D-C1G	100.9(5)
O1-C1-N2	122.6(4)
O1-C1-C1A	122.6(4)
N2-C1-C1A	114.9(3)
C1-N2-C2A	123.3(3)
N2-C2A-C2B2	111.3(4)
N2-C2A-C2B1	108.1(4)
C2B2-C2A-C2B1	109.4(4)
N2-C2A-C2	112.0(3)
C2B2-C2A-C2	109.9(4)
C2B1-C2A-C2	106.0(3)
O2-C2-OT	124.9(4)
O2-C2-C2A	123.1(4)
OT-C2-C2A	111.8(3)
C2-OT-CT1	120.8(3)
OT-CT1-CT2	109.8(4)
OT-CT1-CT4	108.3(5)
CT2-CT1-CT4	115.2(6)
OT-CT1-CT3	102.1(4)
CT2-CT1-CT3	110.7(6)
CT4-CT1-CT3	109.9(5)

Table S10. Selected torsion angles [°] for Z-L-Pro-Aib-O*t*Bu.

C02-C01-C07-OU	32.7(6)
C06-C01-C07-OU	-147.7(4)
C01-C07-OU-C0	170.2(4)
C07-OU-C0-N1	176.2(5)
OU-C0-N1-C1A	-17.5(6)
C0-N1-C1A-C1	-60.0(5)
N1-C1A-C1-N2	168.8(3)
C1A-C1-N2-C2A	175.7(3)
C1-N2-C2A-C2	-53.1(5)
N2-C2A-C2-OT	-31.8(5)
C2A-C2-OT-CT1	-178.5(4)
C2-OT-CT1-CT2	-59.4(6)
C2-OT-CT1-CT4	67.2(6)
C2-OT-CT1-CT3	-176.9(4)

Table S11. Main absorption band maxima (nm) recorded for IT03 in different solvents.

	λ_{max}/nm		
	Band I	Band II	Band III
DMSO	276	316	378
Bidistilled water	272	310	370
Saline solution 0.9% w/v NaCl	261	312	--
PBS	262	313	375
Cell culture medium + 10% bovine fetal serum	273	307	362

*λ_{max} determined soon after dissolution

Table S12. Inhibition potency of selected compounds incubated (1 h for the Au(III) complexes, and 24 h for Cisplatin and Olaparib®) with purified PARP-1. Values expressed in terms of IC_{50} ± st.dev. (μM).

	IC_{50} ± st.dev (μM)
IT03	0.017 ± 0.006
AuL12	0.019 ± 0.004
Cisplatin	12 ± 2
Olaparib®	0.00500 ± 0.00001

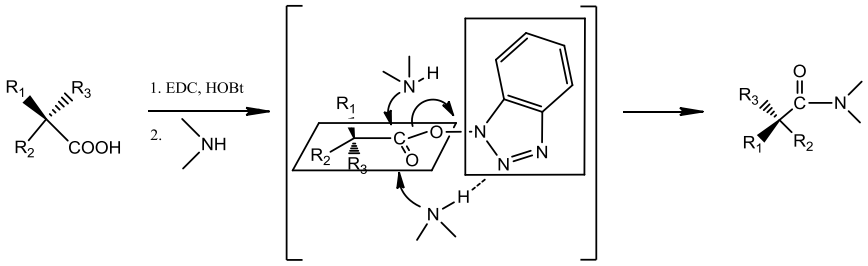

Figure S1. Schematic representation of the peptide bond formation using HOBt/EDC approach.

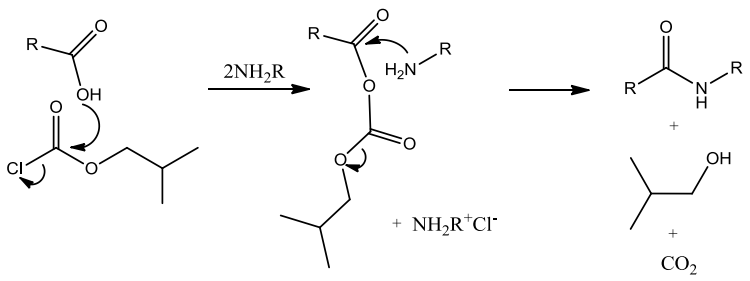

Figure S2. Schematic representation of the peptide bond formation using isobutylchloroformiate as a coupling reagent.

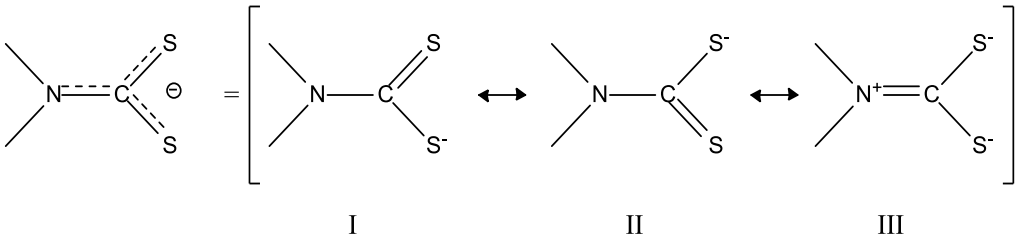

Figure S3. Resonance forms of the dithiocarbamic –NCSS$^-$ moiety.

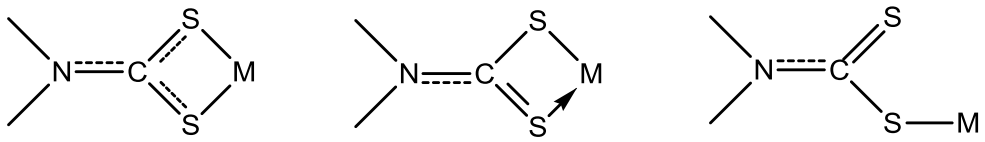

Figure S4. Different ways of metal-sulfur binding in dithiocarbamato complexes: symmetrical bidentate (a), asymmetrical bidentate (b) and monodentate (c).

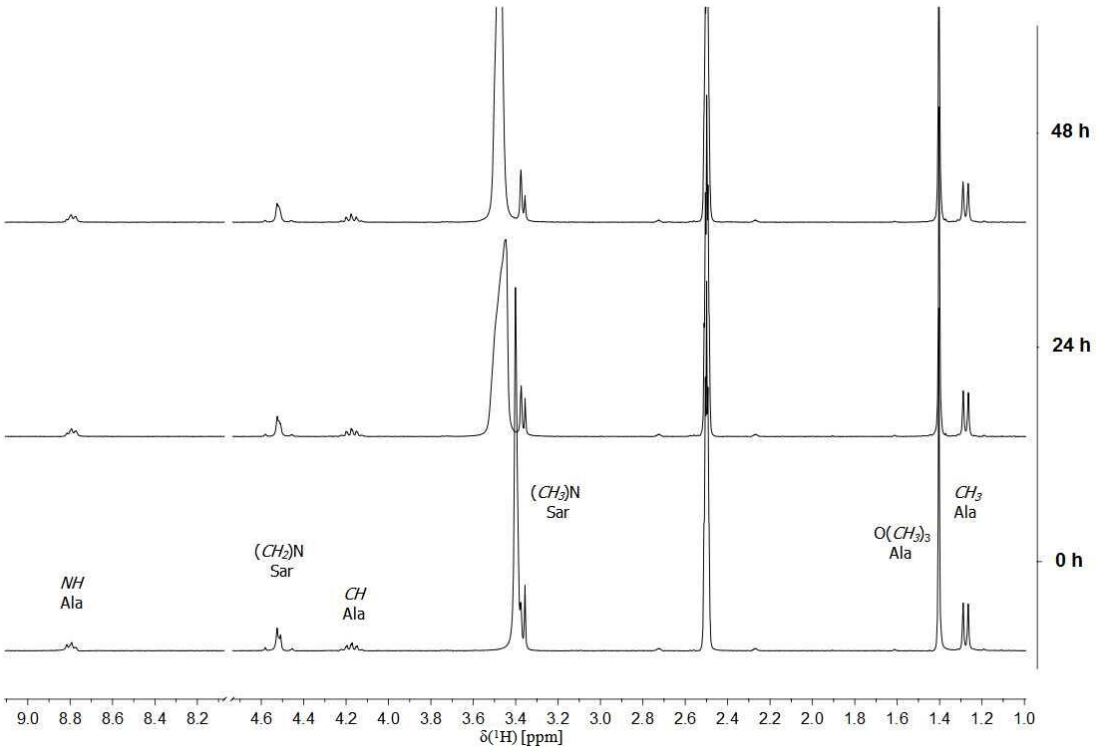

Figure S5. ^{1}H-NMR spectra of IT01 in DMSO-d_6 over 48 h.

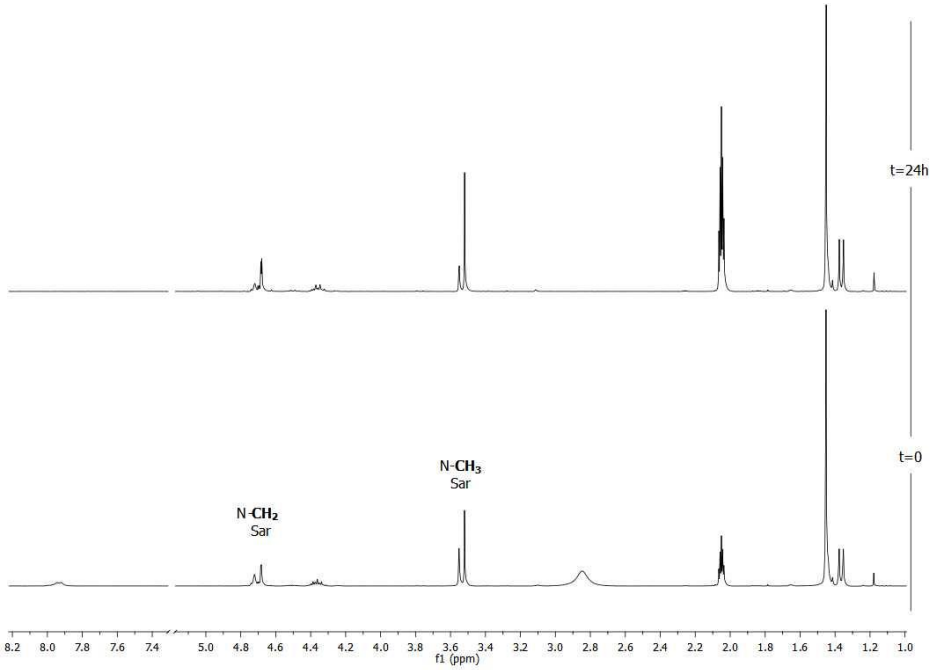

Figure S6. ^{1}H-NMR spectra of IT01 in acetone-d_6 over 24 h.

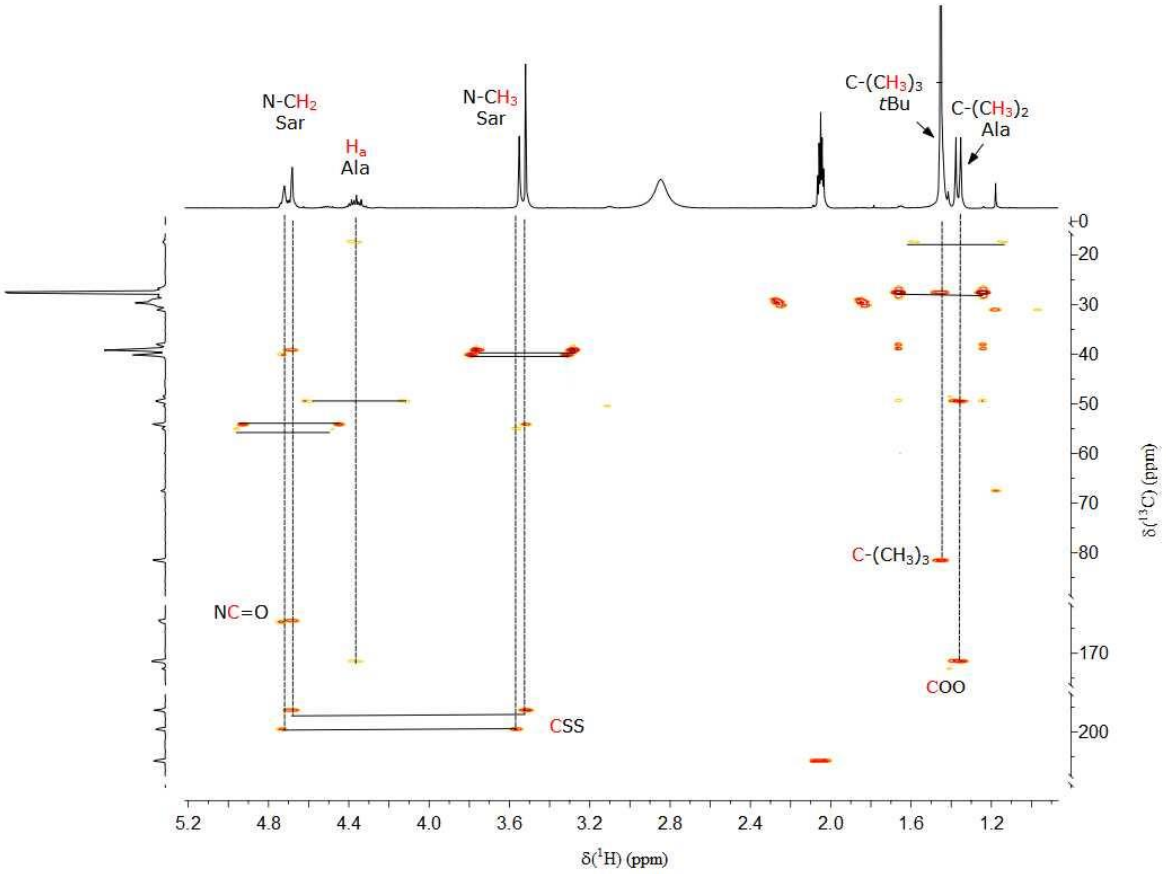

Figure S7. [^{1}H,^{13}C]-HMBC spectrum of IT01 in acetone-d_6.

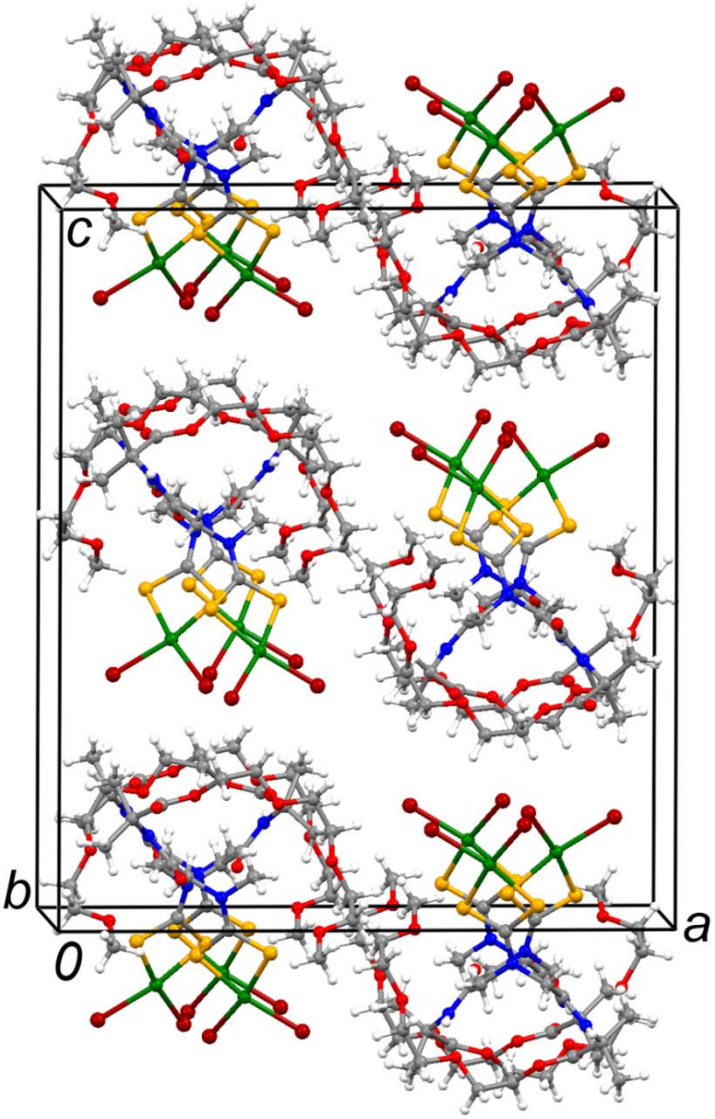

Figure S8. Crystal packing of IT05·pentane viewed along the b crystallographic axis.

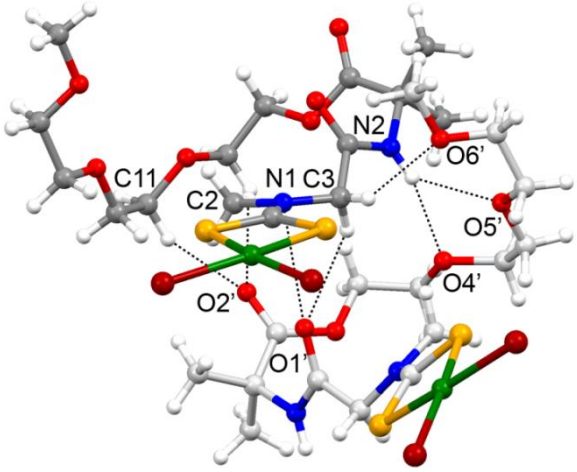

Figure S9. Depiction of intermolecular contacts between two symmetry related molecules of IT05·pentane. Symmetry code ' = 1/2-x; 1/2+y; z.

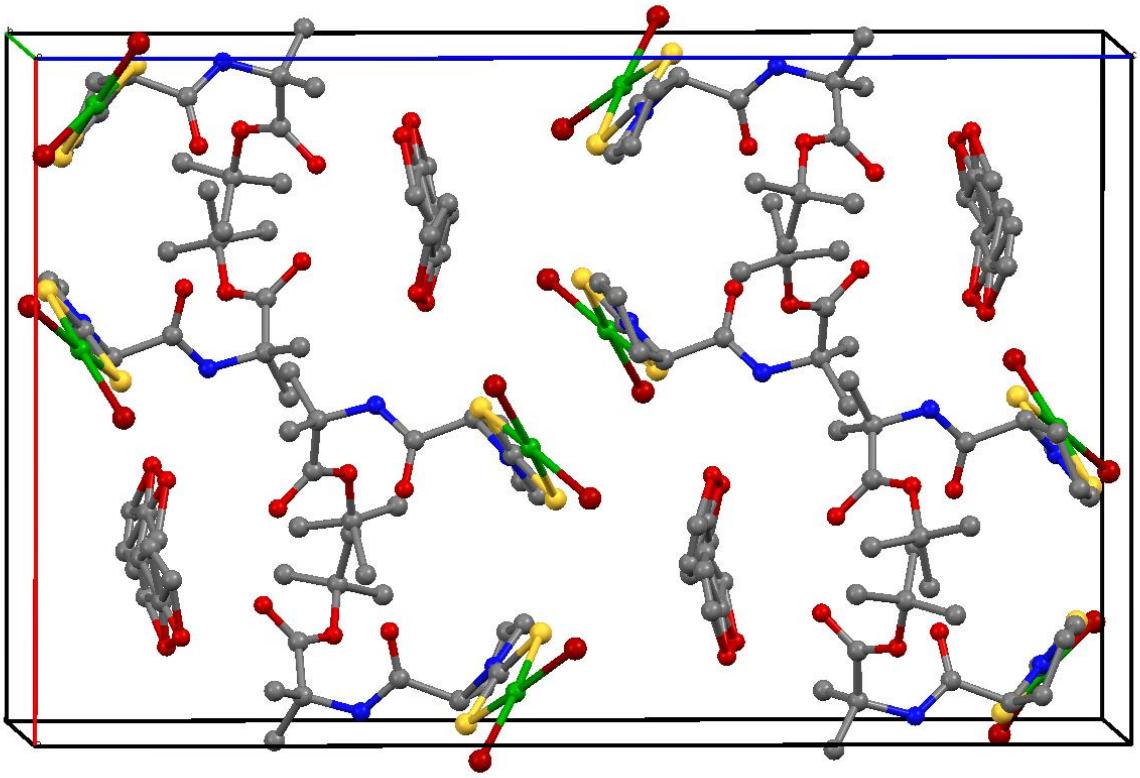

Figure S10. Crystal packing of IT03/IT04 acetone solvate viewed along the b crystallographic axis.

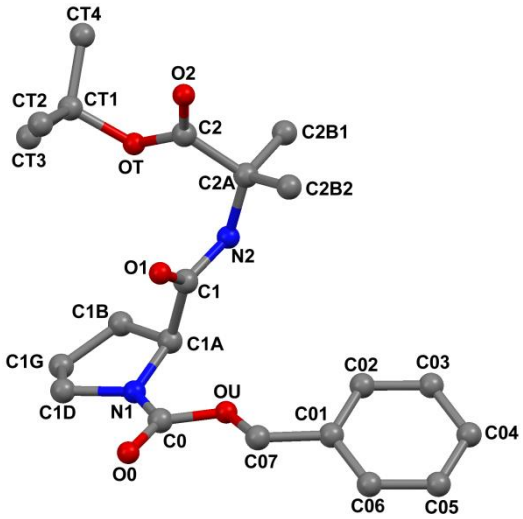

Figure S11. X-ray diffraction structure of Z-L-Pro-Aib-O*t*Bu with atom numbering (only one position for the disordered C1G atom is shown; H-atoms have been omitted for clarity), characterized by a *cis* configuration of the Z-L-Pro urethane bond [the value of the OU-C0-N1-C1A torsion angle being -17.5(6)°], a not uncommon observation for urethane-protected Pro derivatives. The peptide backbone features a *semi*-extended conformation for the Pro residue [ϕ,ψ = -60.0(5)°, +168.8(3)°] while right-handed helical for Aib [ϕ,ψ = -53.1(5)°, -31.8(5)°]. Such a conformation is closely matched by the L-Pro-Aib segment in the structure of the racemate IT03/IT04. In the packing mode, an intermolecular H-bond is observed between the (peptide) N2-H group and the (-*x*, 1/2+*y*, 3/2-*z*) symmetry equivalent of the (urethane carbonyl) O0=C0 group, linking molecules related by a twofold screw axis along the *b* direction.

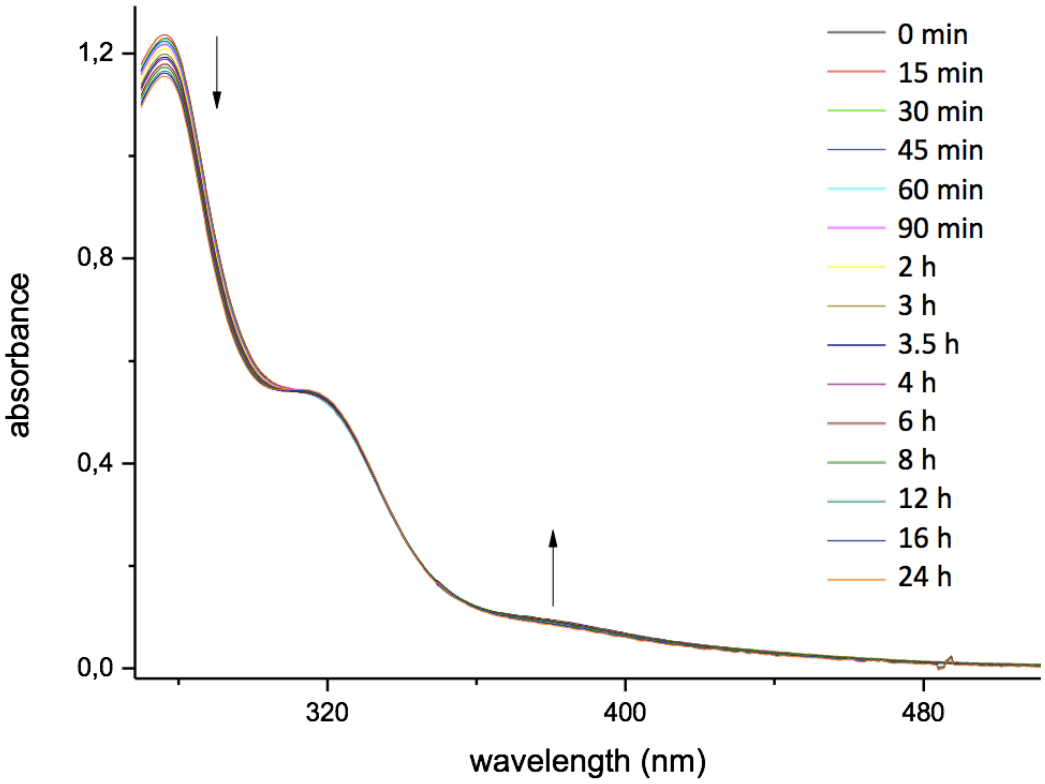

Figure S12. Electronic spectra of IT03 (50 μM) recorded in DMSO at 25°C for 24 h.

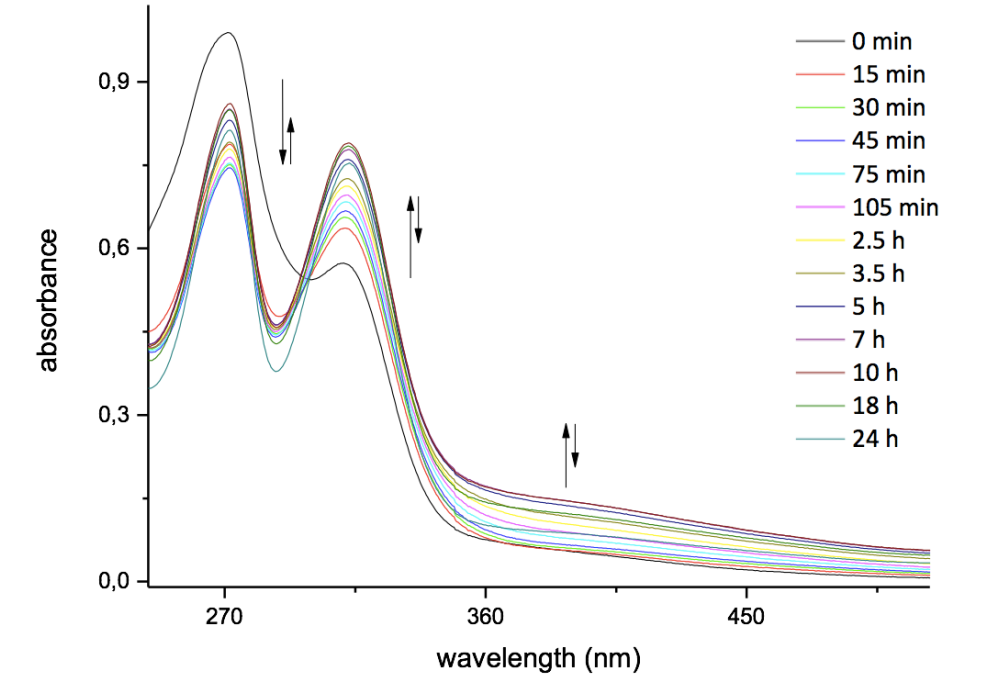

Figure S13. Electronic spectra of IT03 (50 μM) recorded in deionized water at 25°C for 24h.

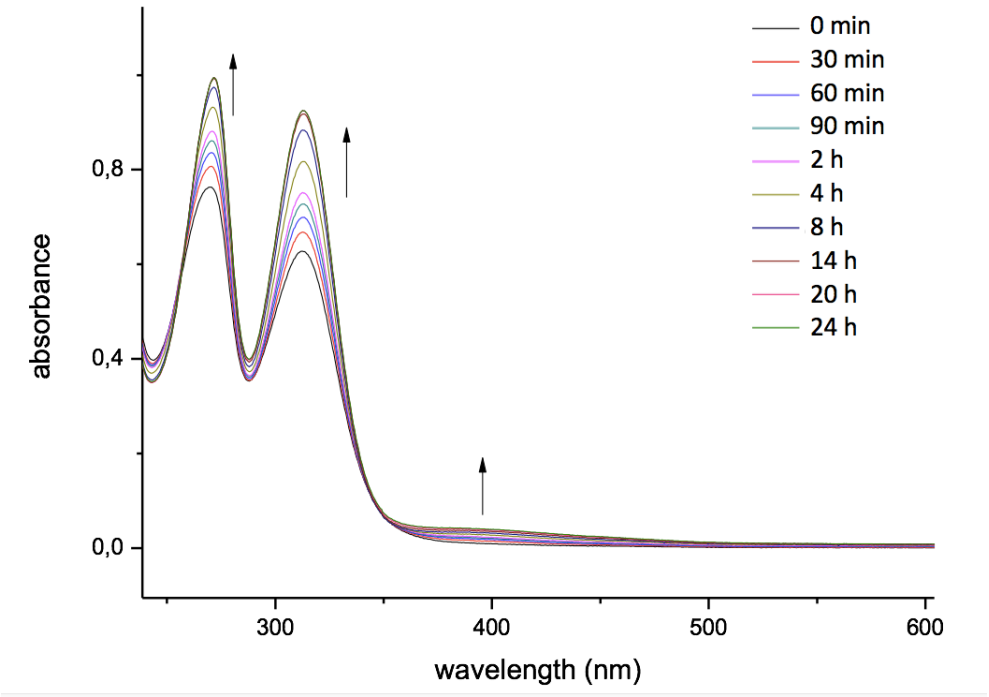

Figure S14. Electronic spectra of IT03 (50 μM) recorded in saline solution (NaCl 0.9% w/v) at 25°C for 24 h.

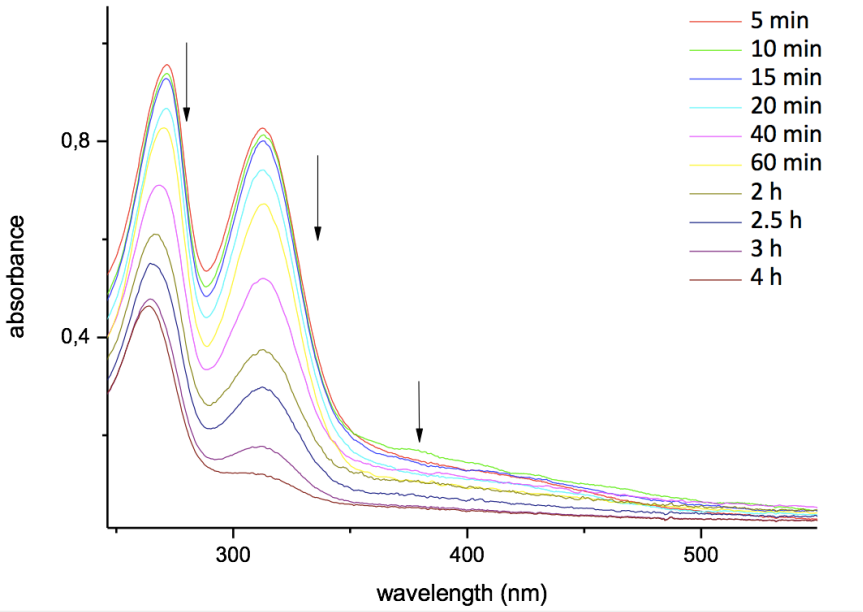

Figure S15. Electronic spectra of IT03 (50 µM) recorded in PBS buffer pH=7.4 at 25°C over 4 h.

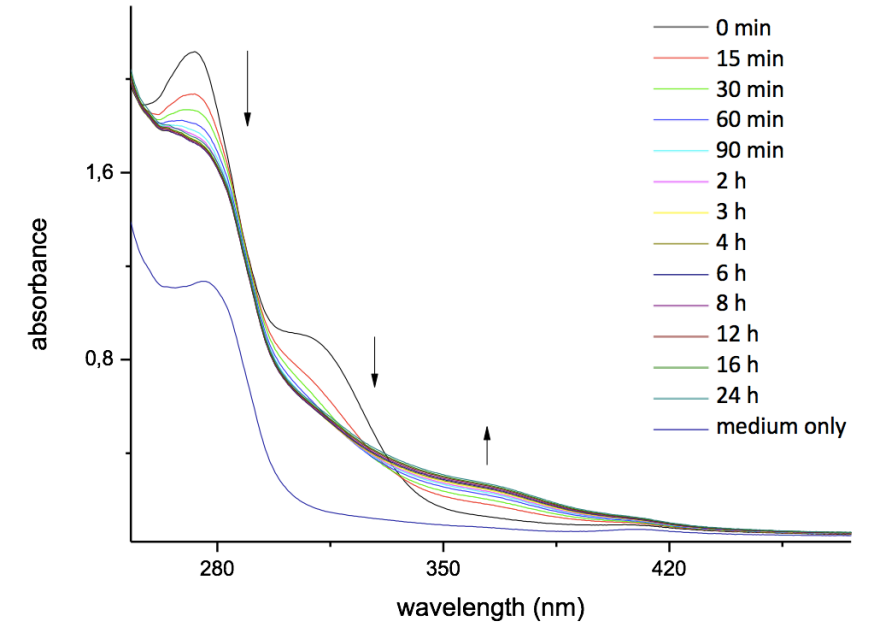

Figure S16. Electronic spectra of IT03 (30 μM) in PBS added of 20% v/v complete medium (RPMI-1640 medium supplemented with 10% fetal calf serum) at 25°C for 24 hours.

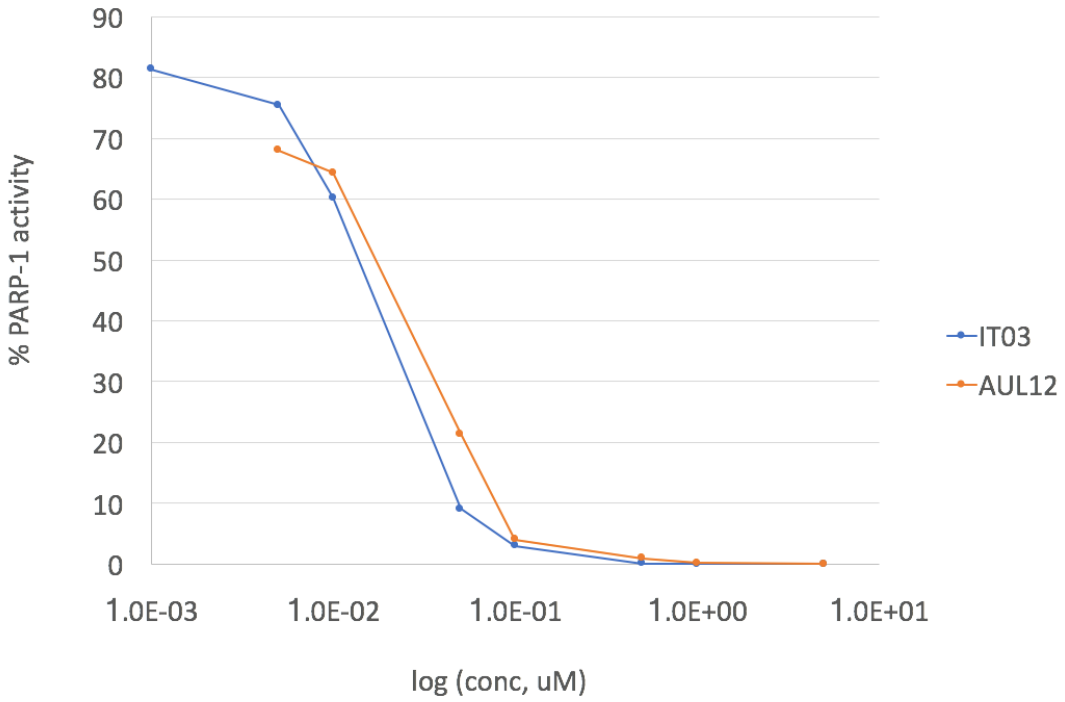

Figure S17. Inhibition of PARP-1 activity by test compounds at different concentrations (from 10 to 0.01 μM). For the assay each compound was incubated for 1 h with 0.5 U of purified protein.

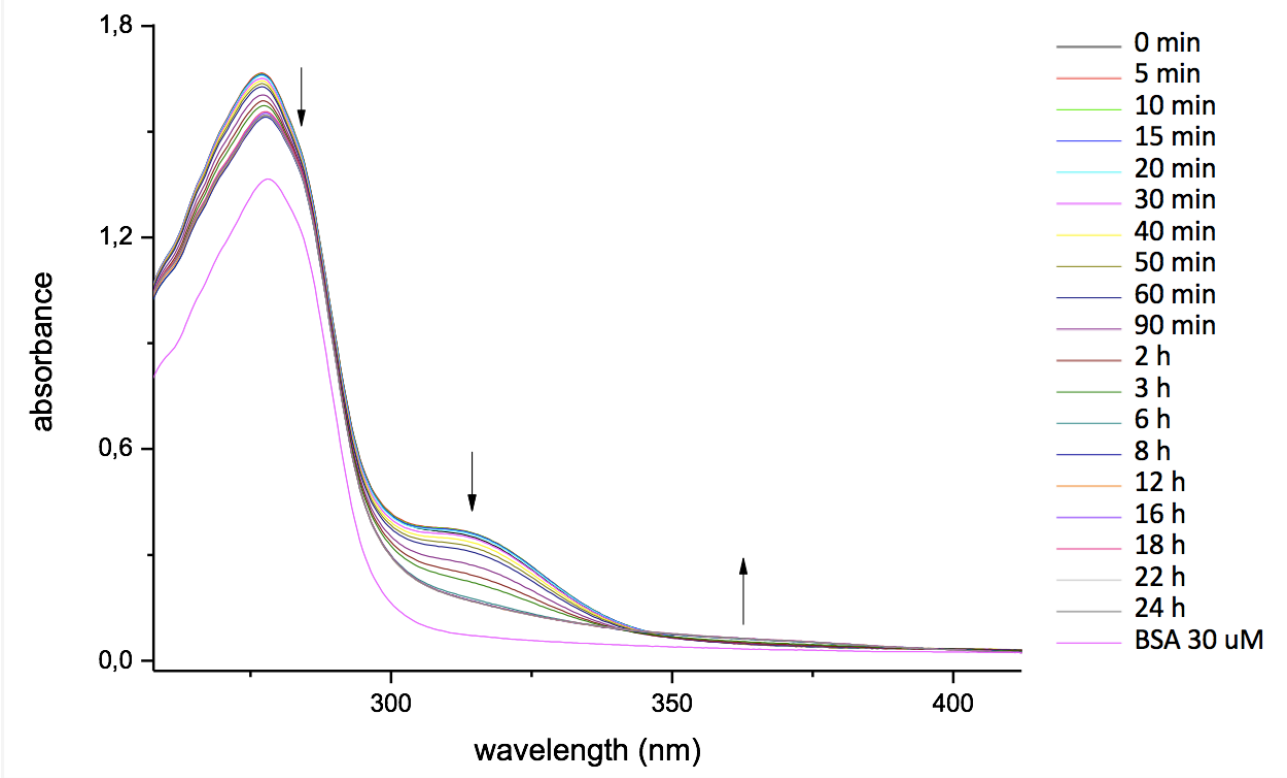

Figure S18. Electronic spectrum of BSA and IT03 (equimolar, 30 μM) in PBS at 25°C over 24 h.

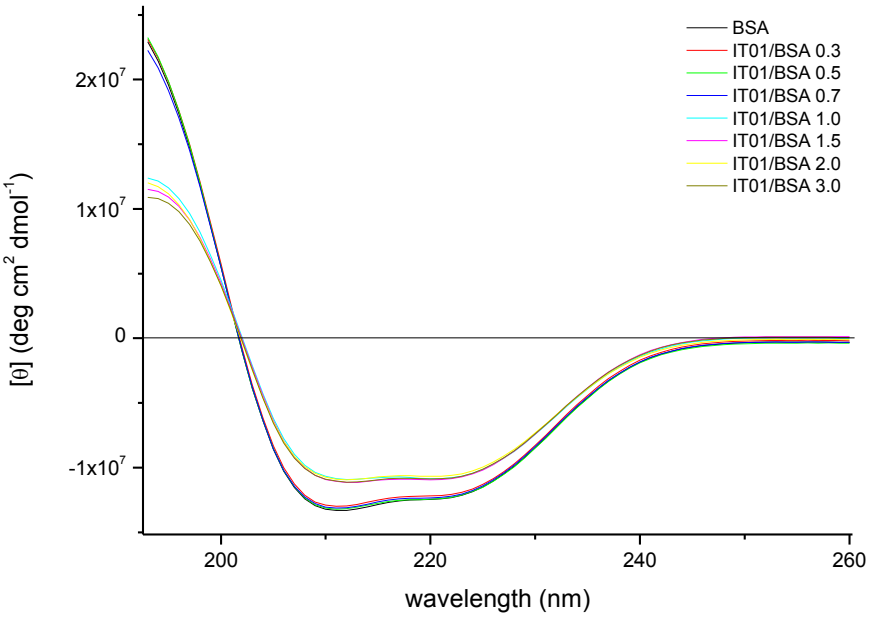

Figure S19. CD spectra of BSA incubated with IT03 at different molar ratios (from 0 to 3) in PBS at 25°C.

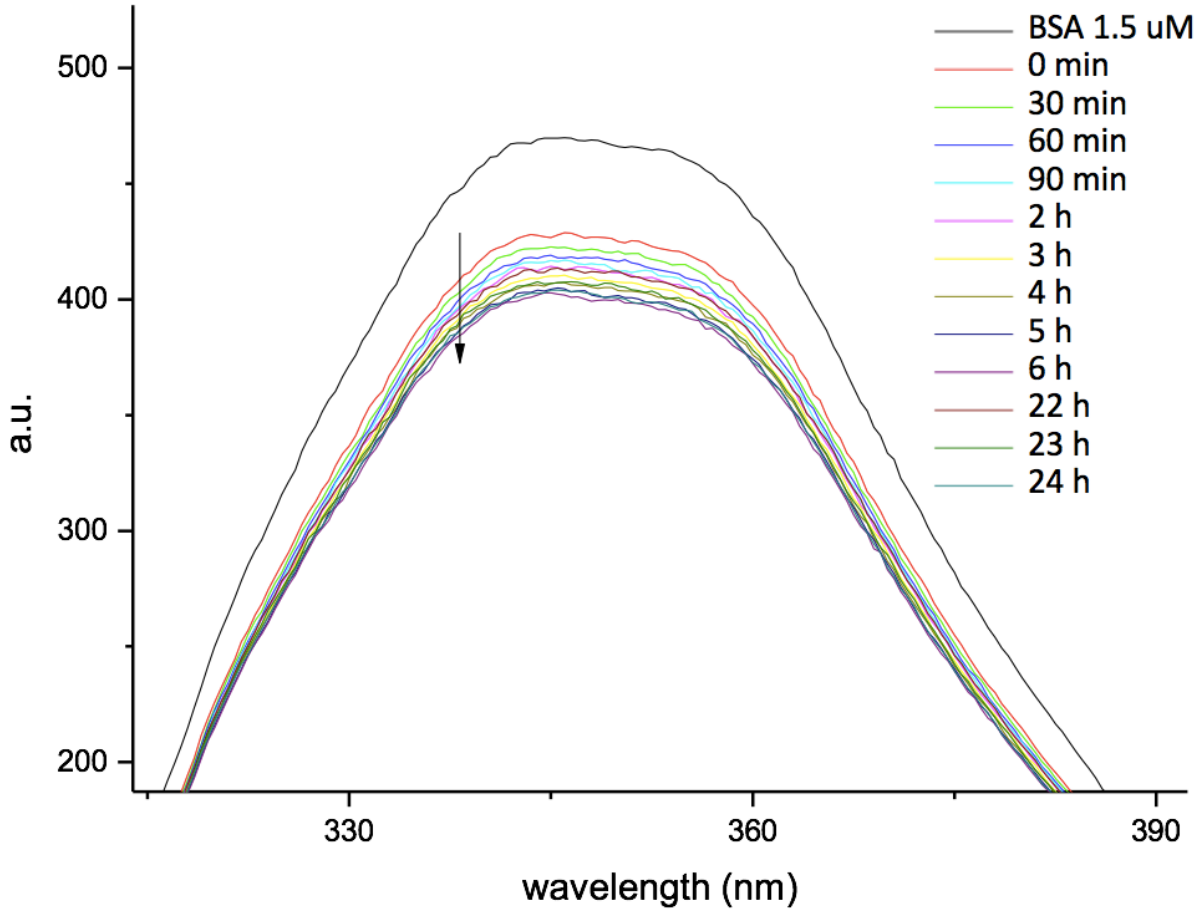

Figure S20. Fluorescence spectra of BSA (15 μM) in presence of IT03 (15 μM) in PBS at 25°C over 24h.

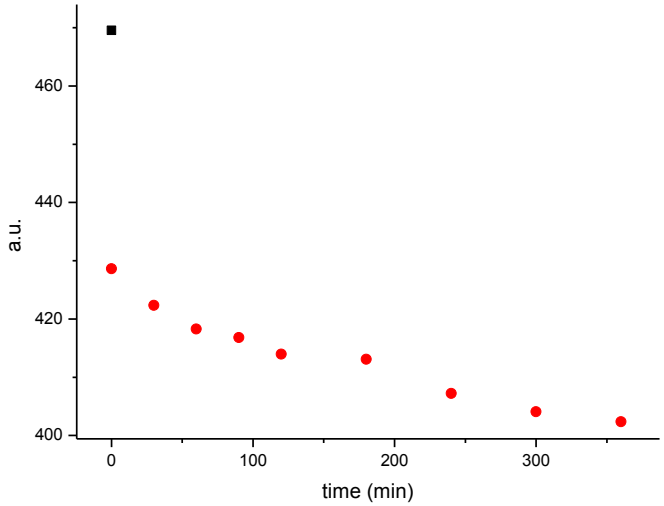

Figure S21. Intensity fluorescence at the λ_{em} maximum (349 nm) of BSA alone (■) and when incubated with IT03 as a function of time (●, 0-6 h).

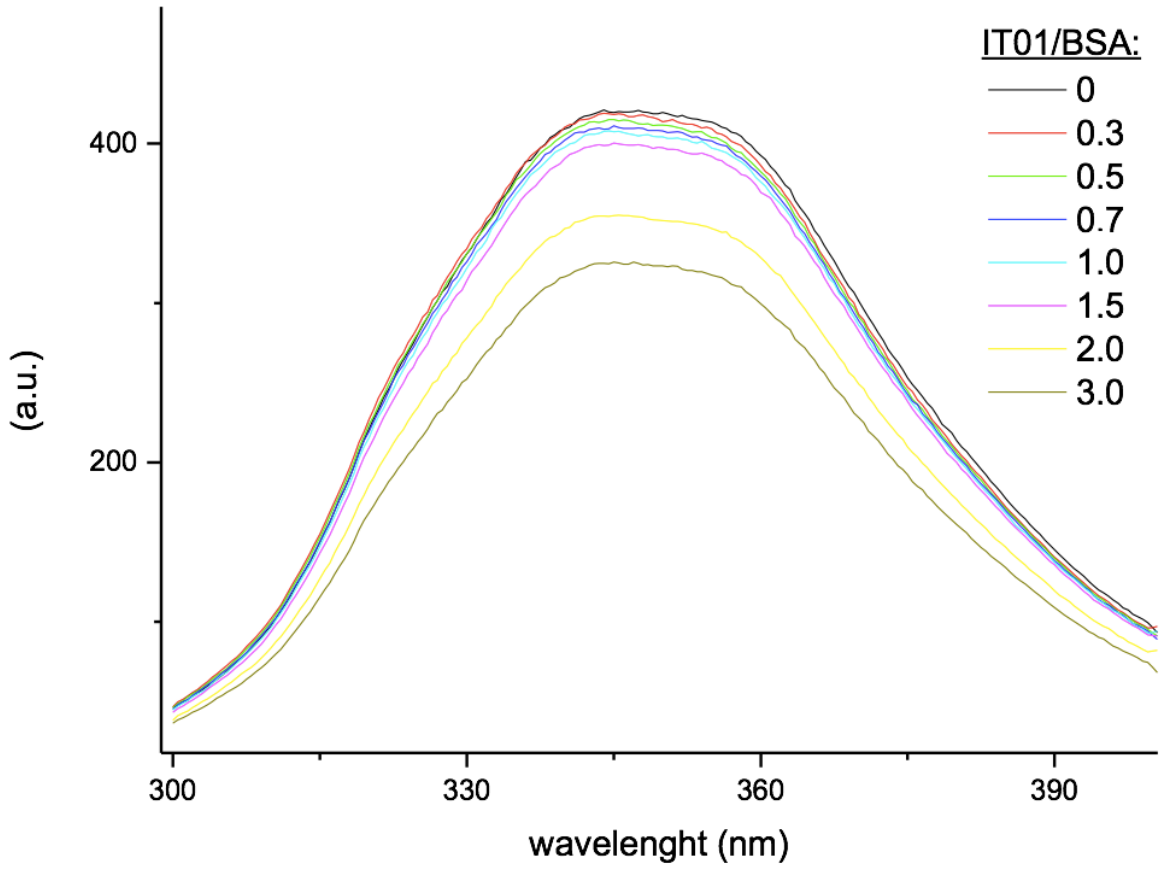

Figure S22. Fluorescence spectra of BSA (15 μM) in presence of IT03 at different molar ratios (from 0 to 3) soon after mixing, in PBS at 25°C.

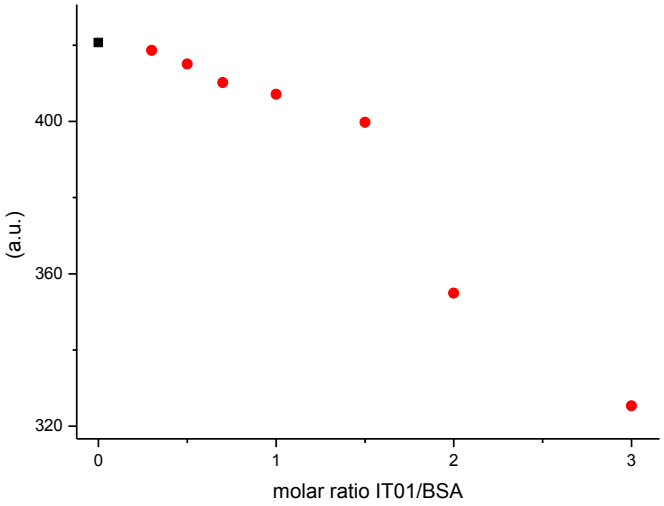

Figure S23. Intensity fluorescence at the λ_{em} maximum (349 nm) of BSA alone (■) and when incubated with IT03 at different IT03/BSA molar ratios (From 0.3 to 3; ●).